Feature profile control and the influence of scan artifacts

Richard Dare[a *], Paul R. Rowlands[a †], Terrence E. Zavecz[b ‡]
[a]Agere Technologies, Orlando, FL
[b]TEA Systems, Alburtis, PA 18011

ABSTRACT

Competitive high volume semiconductor manufacturing yields require that critical feature profiles be continually monitored for uniformity and production control. Historically this has involved long and tedious analyses of Scanning Electron Microscope (SEM) photos that resulted in an average feature profile or a qualitative comparison of a matrix of black and white images. Many factors influence profiles including wafer flatness, focus and film thicknesses. Characterizing profile uniformity as a function of these parameters not only stabilizes high product yields but also significantly reduces the time spent in problem aversion and solution discovery.

Scatterometry uniquely provides the combination of feature metrics and spatial coverage needed to monitor production profiles. The vast amount of data gathered by these systems is not well handled by classic statistical methods. A more practical approach taken by the authors is to apply spatial models to the profile data to determine the relative stability and contributions of film, substrate and the exposure tool to process perturbations.

Recent work performed by Agere and TEA Systems is shown to be capable of quantitatively modeling the relative contributions of lens slit, reticle-scan and lens degradation to feature size and side-wall angle (SWA). This work describes the models used and the slit-and-scan contributions that are unique for each exposure tool.

Finally it is shown that the direction and linearity of the reticle scan can be a contributing factor to the feature profile error budget with direct influence production image stability.

Keywords: Lens, aberration, perturbation, process control, SEM, Scatterometry, scanner, semiconductor, model, wafer

1. INTRODUCTION

The contributions of the exposure tool and wafer process to Intra-wafer linewidth variation were first discussed by Wong et al.[1] Dusa et al followed this groundwork by presenting an algorithmic signature formalization of the intra-wafer aberrations resulting from exposure setup, scan direction, Post Exposure Bake and develop.[2] This work addressed systematic sources of full-profile feature and film interaction behavior as measured by scatterometry metrology. The results of this study demonstrated that after removing the reticle contribution, identified process perturbation components of PEB and BARC thickness as the largest feature-uniformity error components for a typical 90 nanometer (nm) lithography process. According to the same data, the contribution from the exposure tool accounts for less than 20% of process feature perturbations with those from focus and dose comprising approximately 14%.

An algorithmic approach to run-to-run control of scanner focus and dose using in-line metrology was presented by Ausschnitt and Cheng[3]. This methodology independently calibrated the focus-dose control surface of the exposure tool for both profile top and bottom measurements using the inverted dose model of equation <**1:**

$$W = \sum_{m=0}^{M} \sum_{n=0}^{N} A_{nm} \left(1 - \frac{Eo}{E}\right)^{n} F^{m} \qquad <\mathbf{1}$$

Where W is the feature size measurement, F the defocus error and Eo is the desired dose setting that produces the target feature size.

In this work, the coefficients of equation **<1** were stored as a signature description of the process-dose control surface for the tool. The stored model signature is then subsequently applied in a run-to-run feedback control

[*] Currently with Infineon, Richmond, VA
[†] Currently with Intersil, Melbourne, FL
[‡] Contact tzavecz@TEAsystems.com or +(01) 610 682-4146

scenario for feature-localized focus and dose extraction by directing the technique only to isolated* patterns to minimize the isofocal dose response of the image. The method recognizes the disparate monotonic, non-asymmetric simultaneous response of the feature top and bottom signatures to provide analytic solutions to an inversion of the model at any site in the exposure sequence. The relative top and bottom feature widths yielding the solution to the problematical defocus sign determination.

The coefficients of equation **<1** are characterized as:

A_{00}	Bottom feature size at optimum dose and focus
A_{10}	The dose sensitivity or change of features size with dose being inversely proportional to exposure latitude.
A_{20}	Rate of change of dose sensitivity with dose
A_{02}	Defocus sensitivity of the feature
A_{12}	Dose & defocus coupling

and are typically assumed stable for any given process over time and across the exposure field.

1.1. Problem Formalization

Full-profile, scatter metrology comes in the form of wafer spatial maps for each parameter of the model. The variables provided include not only profile descriptors such as feature top, bottom and side-wall-angle but also the film thickness for any of the underlying actinic wavelength translucent layers.

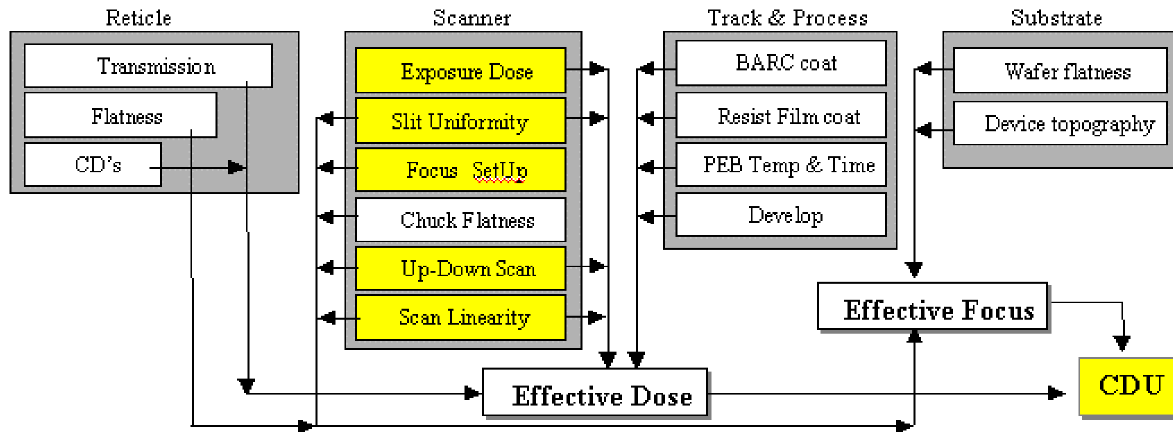

Figure 1: Sources of CD non-uniformity

Perturbations of the nominal dose and focus result in a process variance of Critical Dimension Uniformity (CDU).

The sources of feature profile variation, or Critical Dimension Uniformity, and their contribution to effective dose and focus are shown in figure 1.[4] The effective dose experienced by any localized pattern is the end-point summation of contributions of the reticle, the scanner's optical and electro-mechanical tuning and the slowly changing spatial systematic errors contributed by the track and processing. The scanner sources of focus and dose perturbation are both numerous and critical. Although these sources, for a well-maintained tool, contribute a small portion of the error budget, even a stable tool will experience variations across critical areas of the exposure field. As an example, consider the full-field process window analysis shown in figure 2. Figure 2 presents a composite systematic process window for an 80 nm 1:1 feature. Features from thirty (30) sites across a 24 x 28 mm field are simultaneously tested for a common process window.

Notice in the figure that most of the feature window contours, corresponding to the Upper and Lower Control Limits of the nominal feature size are reasonably well behaved and their response to focus and dose track out to the extremes of focus. The general variation in their actual positioning will be due to the perturbations introduced

* Isolated features are defined as nested patterns whose pitch is equal or greater than twice their nominal width.

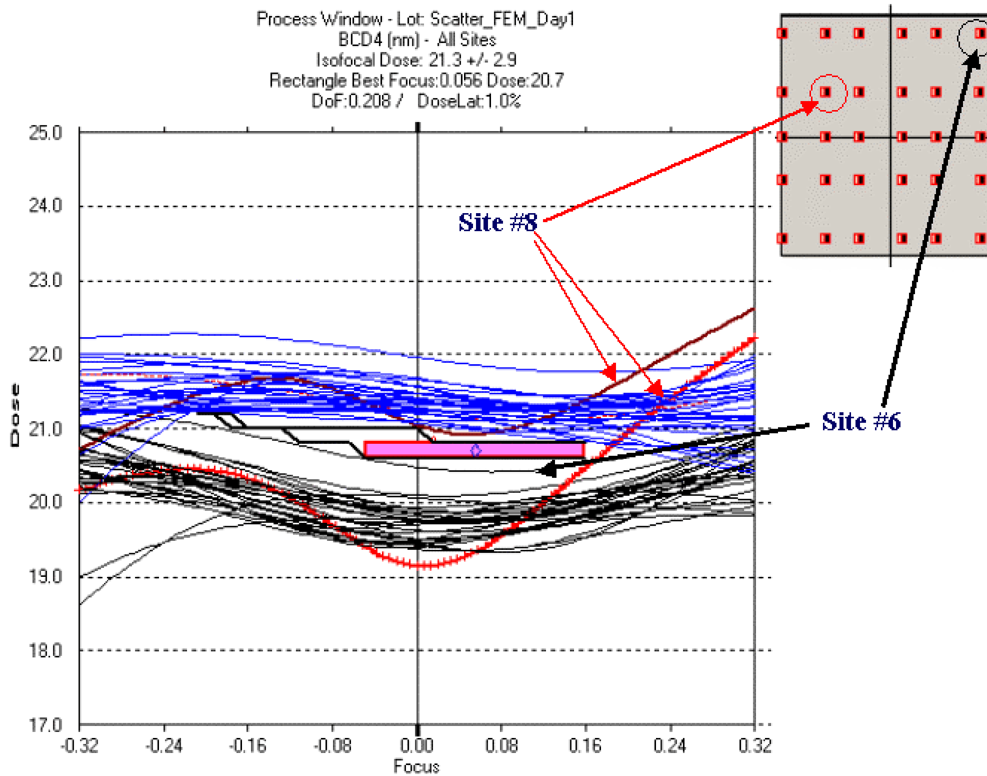

Figure 2: Scanner full-field process window set to 10% Exposure Latitude of 80 nanometer features
This plot is for a family of curves for a reticle and full-field exposure tool performance. Two sites, # 8 and # 6, represent window faults resulting from metrology error and electro-optical perturbations respectively.

by the scanner slit (across lens) uniformity, reticle-scan height variations and the reticle.[1,5] The reticle site-to-site variation is typically recognized as the major contribution to this error budget.

Two very interesting contributors to process CDU appear in the response contours for sites #6 and #8. The contours for site # 8 are biased because of a metrology error that was subsequently culled by the analysis and is therefore not a problem. Conversely, site #6 significantly reduced the focus-dose space of the composite window because of end-of-scan errors and the resulting interaction between the lens and reticle scan-stage. The response of devices in this region of the exposure field represented by site # 6 will pose a serious impact upon product yields.

Errors like these can be found in most well maintained tools. The daily stresses of production will contribute additional errors such as lens and lens–coating degradation and film deposition from out-gassing.

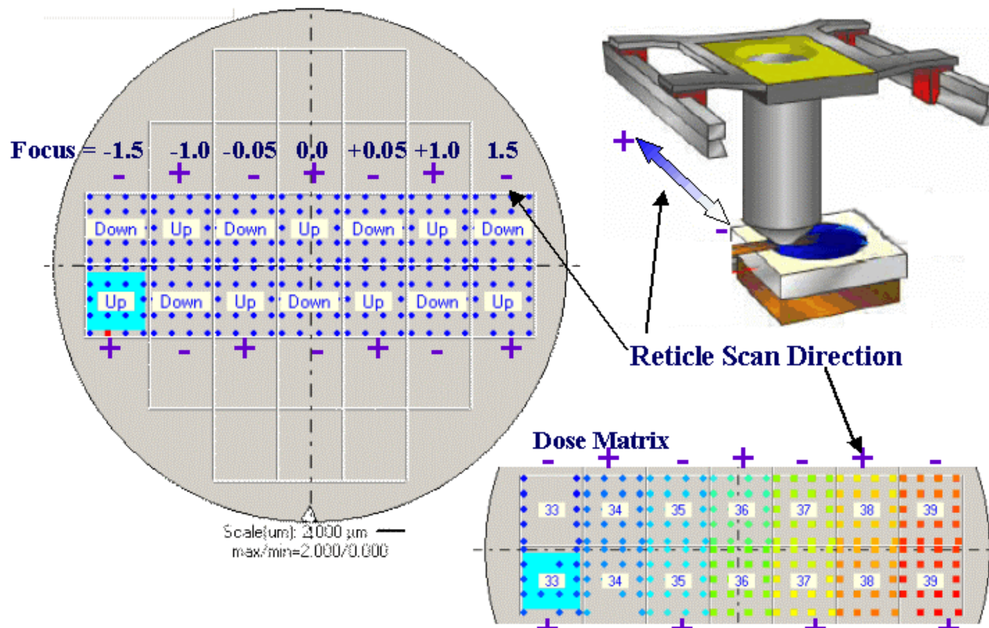

Figure 3: Focus, Dose and reticle-stage scan-direction matrix layouts for the experiment.

1.2. Setup of the Experiment

To detail the influence of some production process window degradation we set up a characterization experiment on a scanner prior to it's scheduled maintenance period. This experiment consisted of:

- Exposure Tool
  - Nikon S204 interfaced to TEL ACT8 coater/ developer
- Film Stack
  - ShinEtsu YD509 Resist on Dielectric ARC on Polysilicon
- Metrology
  - Therma-Wave Opti-Probe 5240
  - Timbre Technologies (TEL) Optical Digital Profilometry (ODP)
- Scheduled Maintenance Action
  - Compare lens performance for before and after cleaning performance
  - Contamination consists of a build up of material on optic just above the wafer. The contamination is removed by gently wiping with lens tissue soaked with water then it is wiped again with methanol.
- Analysis Method
  - Weir PW software from TEA Systems was used for spatial and process window modeling.
  - The algorithm of equation **<1** was used for the process window portion of the analysis along with some data pretreatment for the removal of slowly varying wafer perturbations.

Focus and dose matrices were exposed on two rows of separate wafers as shown in figure 3. The features for this experiment were isolated, as defined by the definition of footnote on the first page of this paper, and consisted of 175 nm vertical lines on a 2;1 duty cycle. A 4x5 matrix of sites across the 24 x 28 mm field were measured Care was taken to insure that the reticle scan-stage followed the scan directions shown in the figure.

Comparative results from both before and after lens cleaning are shown in figure 4, all fields exposed at the optimum dose for the feature. Each column in this analysis allows a direct comparison of reticle-stage scan direction for a given focus value.

The color contour bar for each plot was set with the target feature value residing at mid-scale (green) and the upper and lower control limits falling at the edge of the deep-red and deep-blue coding as shown on the Bottom CD color bar.

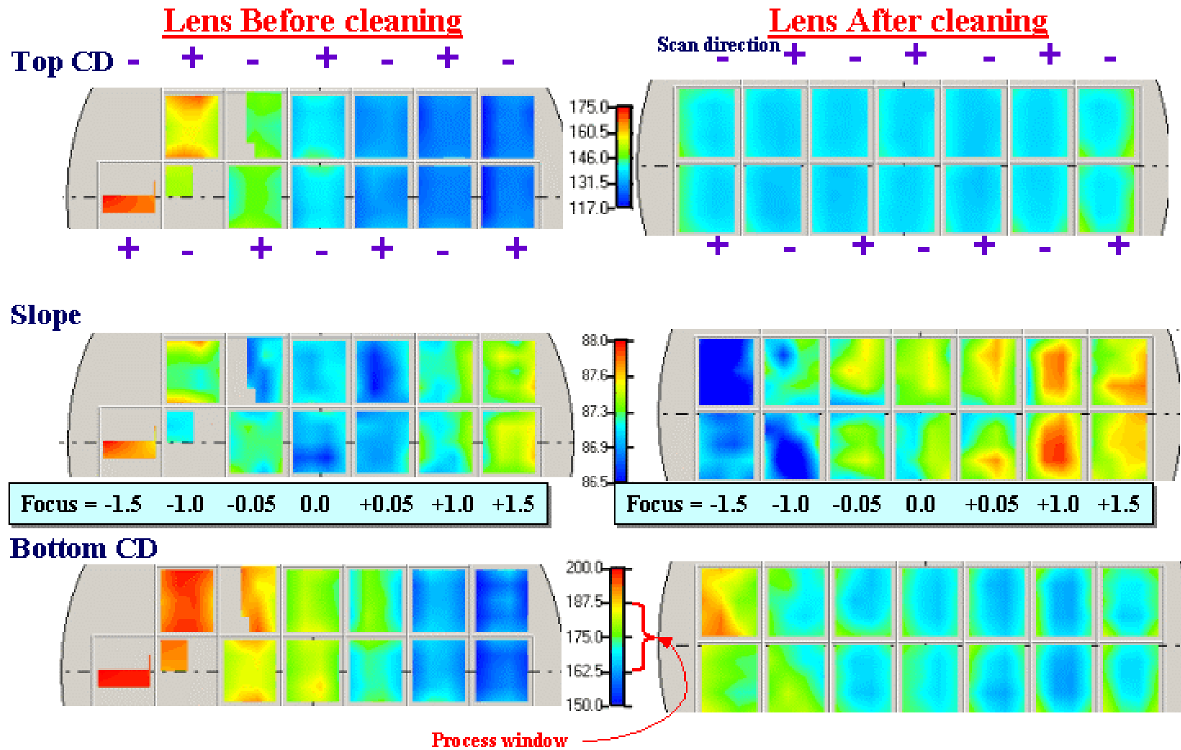

Figure 4: Feature profile perturbations from Focus

The lens response before cleaning contains a number of gray, unexposed regions where either no valid data was gathered or the analysis culled poor metrology points designated with the "Alarm" variable values >1. Notice the asymmetric response of the process. The optimum focus is located at about +0.05 um and apparently remains constant at this value before and after cleaning for the Bottom CD value. Top CD focus however is not as clearly defined and appear to optimize at about the point at which the metrology begins to fail (-0.05 um).

It's interesting to note that the feature slope response to focus has changed character by the lens cleaning. Prior to cleaning, the slopes exhibit a quadratic response to focus while after cleaning, a monotonic variation can be seen. The reduction in depth-of-focus accompanying the lens also belies in a change in the coefficients of equation **<1** associated to the feature response to focus and dose. This behavior suggests that focus-extraction methods that rely on profile slope need to be carefully monitored for stability and exposure response [6,7].

2. LENS AND SCAN INFLUENCE ON THE PROFILE

Wavefront aberrations introduced by the lens are frequently analyzed using a Zernike response model of the phase amplitude in the exit pupil of the optical system.[8] However, the physical construction of the scanner is such that the perturbations of the lens are primarily transferred into an exposure-tool unique lens signature that is replicated on only one Cartesian axis of the image while the reticle-scan induced errors are replicated in the orthogonal axis.

The imaged features therefore see lens induced errors as fixed in their response to local variations in focus. Conversely, the reticle-scan controlled components are closely tied to the uniform motion of the reticle stage and will experience perturbations from the localized focus plus the perturbed, localized dose induced by any residual acceleration of the reticle-stage typically seen at the start or termination of the field scan.[9,10]

The feature variation across the reticle slit can be modeled using a one dimensional series expansion of the

$$WL_j(x) = \sum_{n=0}^{4} a_n x^n$$

<2

form:[11]

Where WL_j is the localized response for feature "j" to the nominal dose (a_o) and lens aberrations (a_1 … a_4). In this one-dimensional response the contributions of the higher orders of the expansion are typically minimal because of the averaging effects of the scan so the equation response is limited to the 4th order. Feature response along the reticle-scan direction is also simplified in this approach with the final feature size for feature "j" characterized by the composite form:

$$W_j(x,y) = WL_j\big|_x + \sum_{m=1}^{6} c_m y^m \qquad <3$$

Here the coefficients c_m characterizes the local perturbations contributed by the tilt and focus errors of the reticle scan stage and Wj describes the final feature size.

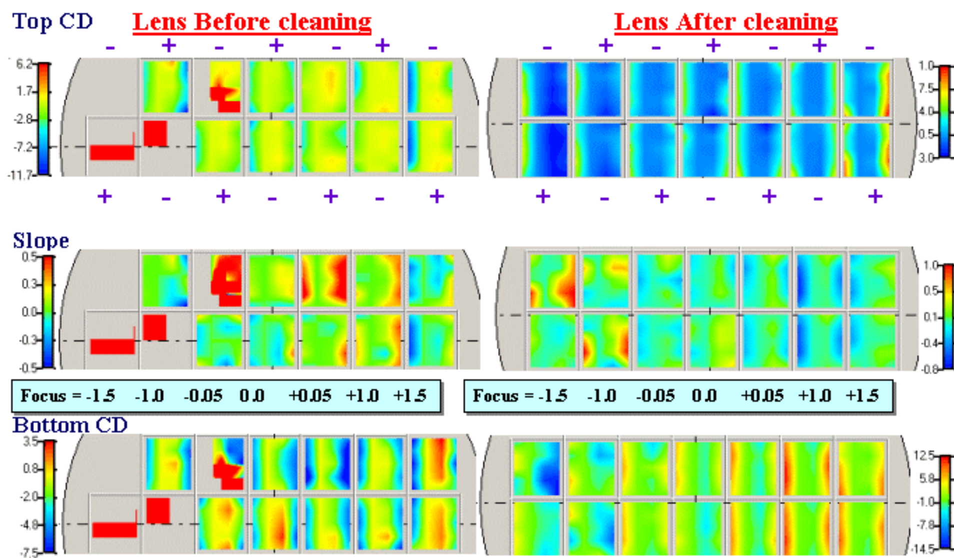

Figure 5a: Lens slit signature stability by removal of the reticle scan signature (+/- = scan direction)

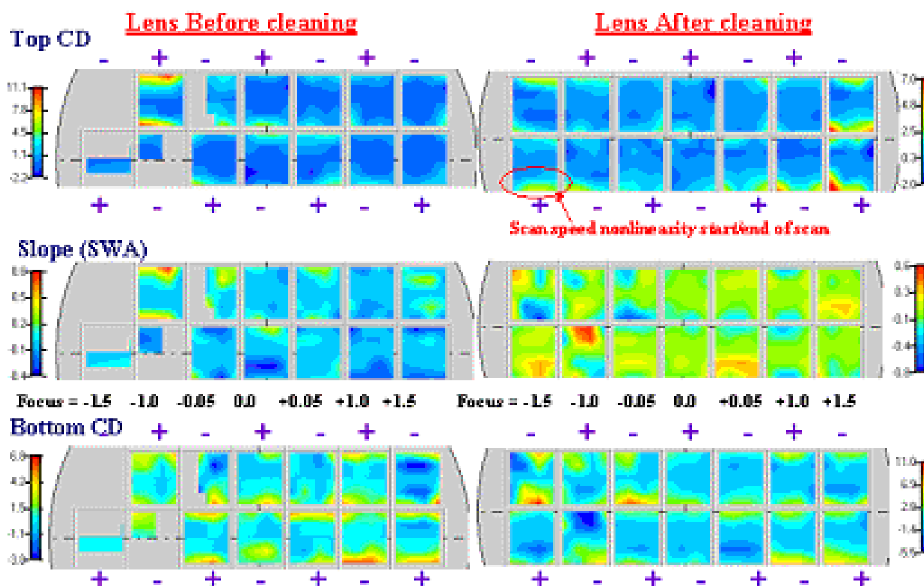

Figure 5b: Reticle Scan-stage signature generated by removal of the lens-slit components.

2.1. Lens-slit signature response

To see the lens slit response stability we took the data set of figure 4 and characterized the reticle-scan signature at each focus. The scan signature component of equation **<3** was then subtracted from the data along with the a_o coefficient to provide a view of the perturbations experienced by the slit in figure 5a.

In the plots of figure 5a, the variations in feature size due to the nominal (localized) dose and defocus have been removed by the removal of the a_o term. The first noticeable factor is the significant change in full-lens response brought on by the cleaning. In an examination of the Bottom CD response, we can see the across-lens curvature on the +0.05 defocus field with a range of 8 nm in a convex surface for the pre-cleaned response changing to a concave variation of more than 12 nm. This could be the result of the out-gassed deposition on the lens acting as a non-uniform neutral density filter or as a new refractive thin-element on the lens.

The Top-CD elements appear to be stable across the focus range, however the Bottom CD feature is experiencing the major changes due to reticle bow fluctuation and localized changes in dose. The slope here is a good indicator of bottom CD fluctuation and the difference in response to the process window.

2.2. Reticle scan perturbations

The analysis then removed the fitted lens signature response of equation **<2** from each field to view the reticle-stage's scan contribution to the feature profile; these results are shown in figure 5b. Again, the influence of the nominal dose and defocus are removed in this analysis by the subtraction of the slit-aberration model. Lens cleaning has not appreciably changed the feature response except for a small improvement in linearity at best focus.

Lens before cleaning

UP +Scan

		Top CD	
Up+	Best Focus	Size_at_BF	DoF
Mean:	0.0740	131.1	0.1870
Max:	0.1570	151.3	0.2600
Min:	0.0000	113.3	0.0930
IFD:	0.1570	38.0	0.1670

		Slope	
Up +	Best Focus	Size_at_BF	DoF
Mean:	0.0240	87.8	0.2570
Max:	0.0580	89.2	0.3270
Min:	-0.0220	86.8	0.1600
IFD:	0.0800	2.4	0.1670

		Bottom CD	
UP+ Scan	Best Focus	Size_at_BF	DoF
Mean:	0.0580	157.5	0.1610
Max:	0.3280	175.2	0.2070
Min:	-0.1170	146.5	0.1330
IFD:	0.4450	28.7	0.0740

Down -Scan

		Top CD	
Down -	Best Focus	Size_at_BF	DoF
Mean:	0.0320	129.8	0.2240
Max:	0.1460	149.2	0.4000
Min:	-0.1010	100.6	0.1200
IFD:	0.2470	48.6	0.2800

		Slope	
Down -	Best Focus	Size_at_BF	DoF
Mean:	0.0030	87.6	0.2130
Max:	0.0490	89.4	0.3530
Min:	-0.0330	85.5	0.0200
IFD:	0.0820	3.8	0.3330

Down -		Bottom CD	
Scan	Best Focus	Size_at_BF	DoF
Mean:	0.0300	158.6	0.2010
Max:	0.5630	185.5	0.3870
Min:	-0.2120	143.5	0.1200
IFD:	0.7750	42.0	0.2670

Figure 6: Profile response statistics for 20 sites at Best Focus (Before lens cleaning)
IFD = Intra-Field feature size Deviation **DoF** = Depth of Focus

Notice that features sizes rise at the end of scan by approximately 7 to 10 nm. This is caused by a difference in scan speed between the stable, central portion of the field and the end-of-scan that results in a change in the effective dose seen by the feature.

2.3. Component observations

The primary observation here is that besides influencing the nominal dose needed to achieve the feature target size, the out-gassing of hydrocarbons and their subsequent deposition on the lens during production will directly influence the system signature aberrations, and therefore the process window response, of the features. The

across-slit lens signature is stable across the defocus range as is the reticle scan.

Reticle-stage scan speed variations results in changes in effective dose that can be observed at the ends of the scan.

Finally, an examination of figures 4, 5 and 6 while noting the scan-direction of the reticle stage quickly leads us to the conclusion that there is a contribution to the feature profile. To quantify this difference, we must identify the response of the image to the process window for each scan direction.

3. RETICLE-STAGE CONTRIBUTED PROFILE PERTURBATIONS

3.1. Algorithmic Formalization

A slight modification of equation **<1** will allow us to evaluate the image without the masking aberrations induced by defocus and the scan:

$$Wj = \sum_{m=0}^{M} \sum_{n=0}^{N} A_{nmj} \left(1 - \frac{Eo}{E}\right)^{n} F^{m} \qquad <4$$

Where Wj is the feature size for the j'th feature located at (Xj, Yj) on the reticle.

Figure 6 displays the statistics of the feature response at Best Focus for the lens before cleaning and the post-clean results are shown in figure 7. The dose selected for feature size and Depth of Focus (DoF) was the process window dose originally determined to produce a 175 nm feature for this process. As a result, the nominal feature sizes at best focus differ for pre- and post-clean.

UP +Scan — **Lens After cleaning** — **Down -Scan**

Up+	Best Focus	Top CD	DoF
Mean:	0.0010	142.5	0.3810
Max:	0.0710	159.0	0.4000
Min:	-0.0460	121.2	0.3130
IFD:	0.1170	37.8	0.0870

Down -	Best Focus	Top CD	DoF
Mean:	-0.0240	144.2	0.3720
Max:	0.0640	173.0	0.4000
Min:	-0.1870	119.7	0.2330
IFD:	0.2510	53.3	0.1670

Up +	FocusSlope	Slope	DoF_Slope
Mean:	0.0180	87.6	0.2150
Max:	0.1190	88.7	0.4000
Min:	-0.0700	86.4	0.0470
IFD:	0.1890	2.3	0.3530

Down -	FocusSlope	Slope	DoF_Slope
Mean:	0.0340	87.5	0.1480
Max:	0.1530	88.9	0.3470
Min:	-0.0520	86.5	0.0270
IFD:	0.2050	2.4	0.3200

Up +	Best Focus	Bottom CD at BF	DoF
Mean:	0.0080	171.6	0.3850
Max:	0.0870	183.2	0.4000
Min:	-0.0710	163.5	0.3330
IFD:	0.1580	19.8	0.0670

Down -	FocusBCD	BottomCD at BF	DoF_BCD
Mean:	0.0160	174.0	0.3350
Max:	0.0750	216.8	0.4000
Min:	-0.0400	157.3	0.1470
IFD:	0.1150	59.5	0.2530

Figure 7: Profile response statistics for 20 sites at Best Focus (After lens cleaning)
IFD = **Intra-Field feature size Deviation** DoF = **Depth of Focus**

3.2. Visualizing the Optimum Feature Field

The coefficients as determined for equation <4 can use the data from each feature to calculate the optimum focus across the field for each site on the reticle. Optimum focus occurs as the point where the first derivative of the features curves with respect to focus is zero. Figure 8 plots the focus as determined by each of the variables of Top CD, slope and Bottom CD. Figure 8 scales are optimized to show focus deviations. The mean focus for each derivative is within the experimental error of 30 nm. Precision will of course be better for isolated features than it

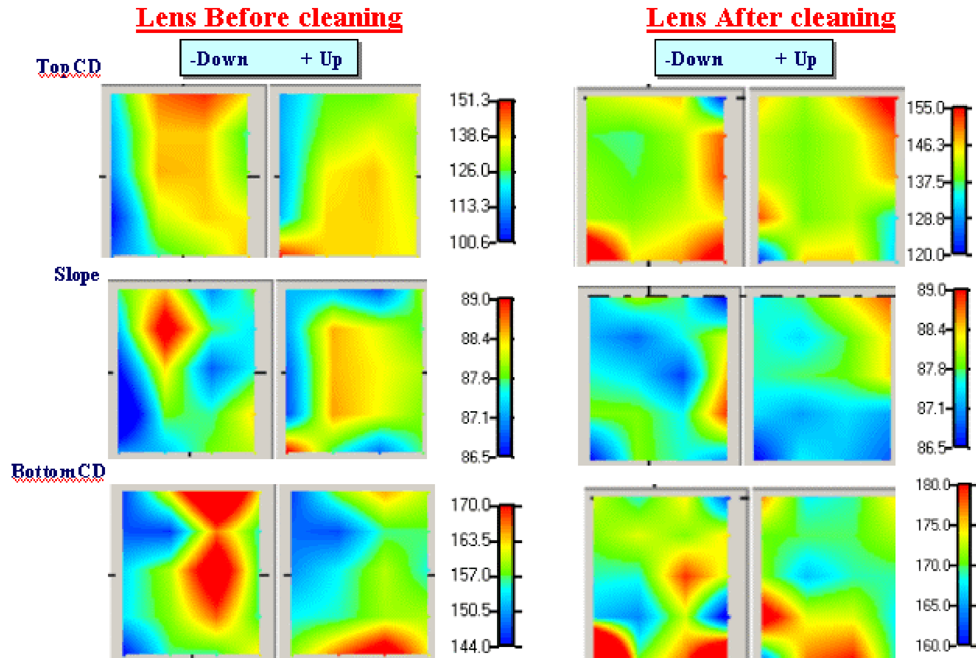

Figure 8: Best Focus as determined by each profile variable

will for dense.

The contour plots of Figure 9 display the optimum CD at best focus and process dose for the tool. The unique characteristic of this plot is that they are contour plots of feature size independent of the perturbing influences of exposure tool focus offset and localized lens/scan defocus.

The lens before clean exhibits the convex lens signature introduced by the contamination. The feature sizes also show a high point in feature size at the start of scan than gradually diminishes to a more-uniform distribution. This bias is caused by residual acceleration of the reticle-scan stage that results in dose biasing at the start of scan.

A much more uniform feature distribution is seen after cleaning the lens but there appears to still be some

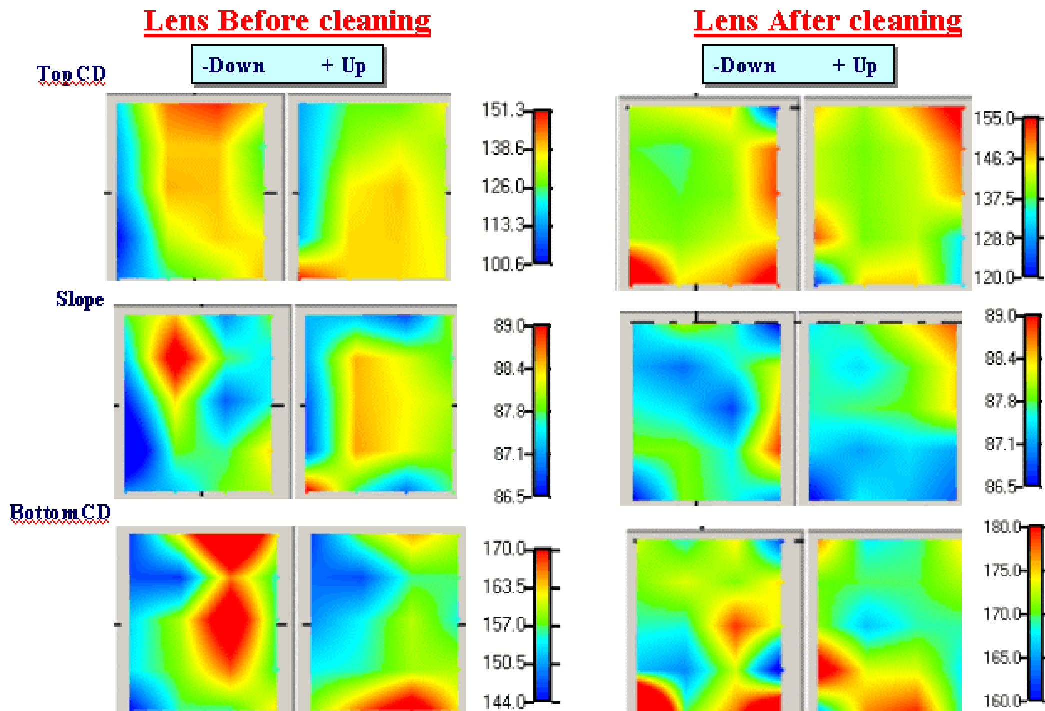

Figure 9: Feature profile uniformity after removal of defocus errors.

remaining scan-speed induced artifacts. The lower left corner of the field also behaves quite differently than that of the remaining exposure and the effects of this are noted in the Depth-of-focus contour plots of figure 10.

The Depth of focus is determined by calculating the range of focus over which the profile feature stays within the upper and lower control limits at the process dose. In figure 10, we can see a improvement in the depth of focus for the lens after cleaning and a very significant performance difference based upon scan direction.

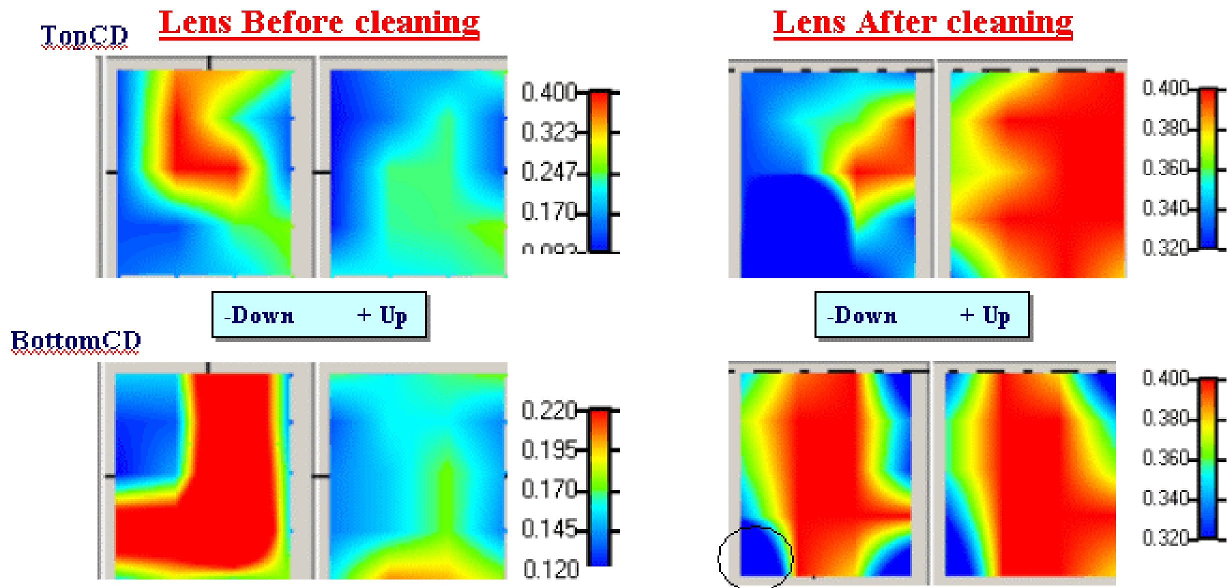

Figure10: Depth-of-Focus (DoF) contours across the field
The area located at the lower left side of the lens --shown encircled-- exhibits markedly lower depth of focus and represents a region of lower process device yield for this exposure tool

3.3. Precision of the analysis method

This analysis method is highly reproducible and this can be seen in the lens/slit signature plot of figure 11.

Data plotted in figure 11 plots the results of the fitting the polynomial of equation <**2** to the matrix. The ordinates of the before and after cleaning graphs are plotted to the same scale. The abscissa represents horizontal location within the slit. A series of box-plots were added to the graphic to allow us to plot the median of each columnar distribution.

For the pre-cleaned lens – left side of figure -- we plotted the medians across the slit for the –Down reticle scan and connected them with a red line. The red median line was then duplicated and translated to the +Up scan of the exposure. As we can see, the first two column medians match within less than a nanometer while the right-most column differ by a maximum of 10 nm.

After cleaning – right graph of figure 11 – the overall curve has shifted up to the nominal process level and all median differences are less than 5 nm.

This method of analysis has provided the photo-processing group with the ability to comparatively monitor up/down and across reticle field line size and shape response across several scanners. This analysis provided support for specific tool usage for critical layers such as gate and also data to communicate with service engineers on issues of uniformity and scan optimization. Regular application of this technique was found to improve scanner performance and increase yield when used as a monitor for scanner performance.

4. CONCLUSIONS

Feature response artifacts from the slit and reticle scan cannot be resolved using only spatial models. However, by varying focus and dose under controlled conditions and the subsequent application of profile-based spatial models, the full-field feature profile can be quantitatively analyzed.

Reticle scan stage perturbations are introduced by both the defocus-height errors of the stage and by scan speed nonlinearity. Residual acceleration of the stage at the start or end of scan will result in 2 to 8 nm of BCD variation

SWA is stage-speed dependent and can result in 0.6 or more degree of variation. Lens cleaning does not strongly improve SWA.

Across-lens or slit perturbations can be observed by removing the modeled reticle scan of each field. Lens perturbations were shown here to contribute +/- 1 degree of SWA and up to 14 nm of BCD variation.

Full-field profile perturbations actually increased in range after lens cleaning but exposure, DoF and process latitude improved.

Scan direction can contribute as much as 42 nm difference in focus, resulting in 28 nm difference in the average Bottom CD measurement. The influence of scan direction is more strongly observed as the lens ages or gathers hydrocarbon residue from exposure to product wafers.

Slit Response signature remains constant with lens aging but the exposure latitude and depth-of-focus degrade. This sensitivity results in greater sensitivity to reticle scan variations.

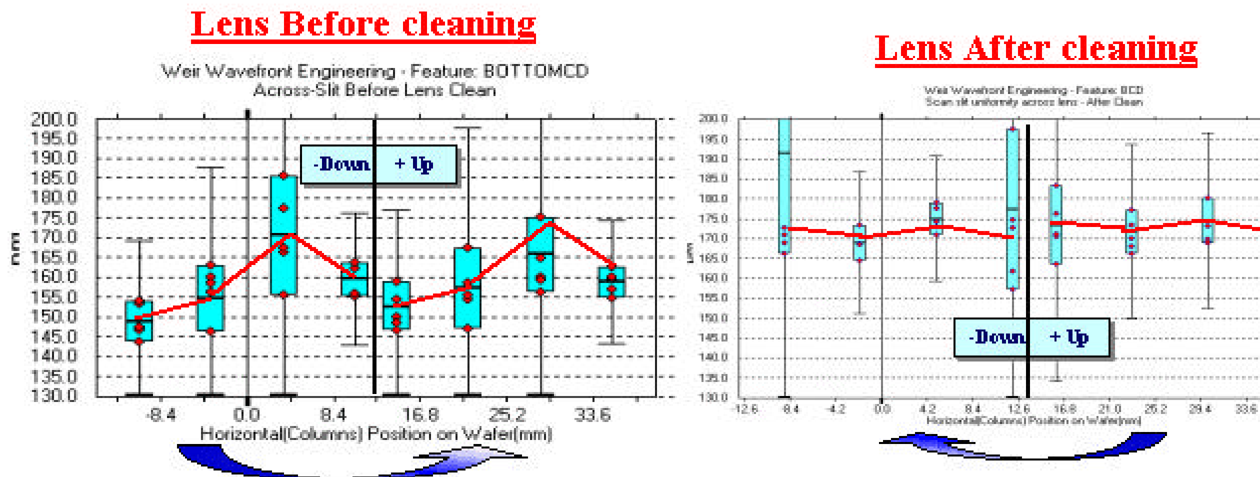

Figure 11: Lens slit signature showing the repeatability of BCD perturbations across the slit.
Lens Before Cleaning (left): The Down-scan median is superimposed on the up-scan
Lens-After Cleaning (right): the Up-scan median is superimposed on the down-scan curve

ACKNOWLEDGEMENTS

The authors would like to thank Brian Swain of Timbre Technologies for his help in developing the ODP models for the scatter metrology.

REFERENCES

1. Alfred Wong, Antoinette Molless, Timothy Brunner, Eric Coker, Robert Fair, George Mack, Scott Mansfield,, "Characterization of line width variation", Proc. SPIE Vol. 4000, Optical Lithography XIII, 184 -191, **2000**

2. Mircea Dusa, Richard Moerman, Bhanwar Singh, Paul Friedberg, Ray Hoobler, Terrence Zavecz, "Intra-wafer CDU characterization to determine process and focus contributions based on Scatterometry Metrology", Proc. SPIE (2004), Vol. 5378-11

3. C. Ausschnitt, S. Cheng, “Modeling for Profile-Based Process-Window Metrology”, SPIE (2004) vol. 5378, pp 38 – 47
4. op.cit.2
5. H. Y. Liu, et all, “Contributions of stepper lenses to systematic CD errors within exposure field”, Proceedings SPIE Optical Lithography, Santa Clara, CA 1995
6. K.Peters, M.Creighton, “Monitoring lithography product data for real-time focus control”, Microlithography World, Nov. 2004
7. op. cit 3
8. J.Kirk, “Review of photoresist-based lens evaluation methods”, Proc of SPIE (2000) , Vol. 4000, pp.1-8
9. T. Zavecz, P.Reynolds, C.Sager, V. Velanki, “The flight of the scanner slit”, Microlithography World, Aug. 2004, pp. 12-16
10. B.Roberts, M.McQuillan, N.Louka, T. Zavecz, P.Reynolds, M.Dusa, “Critical evaluation of focus analysis methods”, Proc. of SPIE (2004) Vol. 5377-207
11. T. Zavecz, “Full-field feature profile models in process control”, Proc. of SPIE (2005) Vol. 5755-16